Thermal Degradation Analysis of the Isocyanate Polyhedral Oligomeric Silsequioxanes (POSS)/Sulfone Epoxy Nanocomposite

Yie-Chan Chiu,[1] Hsieh-Chih Tsai,[2] Toyoko Imae[2,3]

[1]Plating Technology Development Department, Chipbond Technology Corporation, HsinChu, Taiwan 30078, Republic of China
[2]Graduate Institute of Applied Science and Technology, National Taiwan University of Science and Technology, Taipei, Taiwan 10607, Republic of China
[3]Department of Chemical Engineering, National Taiwan University of Science and Technology, Taipei, Taiwan 10607, Republic of China

ABSTRACT: The sulfone epoxy (SEP)/polyhedral oligomeric silsesquioxane (POSS) nanocomposite contains bulky POSS side chains was studied in this research. Its glass transition temperature (T_g) decreases with the bulky POSS content, indicating that the bulky POSS side chains could not only generate the oligomers but also interrupt the network architectures of SEP. Homogeneous and uniform dispersion of POSS in SEP matrix can be obtained through the carbamate/oxazolidon covalent linkage, which is evidenced by scanning electron microscopy. The increasing concentration of POSS into SEP exhibits an increase of char yield in the nanocomposites, indicating that the POSS segments provide the antithermal-oxidation effect for SEP/POSS, thereby inhibiting thermal degradation under open air at high temperatures. © 2011 Wiley Periodicals, Inc. J Appl Polym Sci 124: 1234–1240, 2012

Key words: nanocomposites; thermal properties; TGA; thermogravimetric analysis

INTRODUCTION

The polyhedral oligomeric silsesquioxane (POSS) possesses the chemical formula $[RSiO_{1.5}]_8$, with R represents various organic groups, such as the hydroxyl group, alkyl group, aromatic ring, and so forth. Additionally, the POSS architecture with the sizes of 1–3 nm consisted of well-defined nanoscale inorganic silica-like core.[1–3] The POSS structure and rigidity of the organic tethers cubes could improve the thermal stabilities, higher glass transition temperature, and mechanical properties, and so forth.[4,5] Various polymer materials have been modified by the nanoscale POSS, such as polyimide,[6] polymethymethacrylate,[7] polyurethane,[8] polystyrene,[9] and so forth.

Epoxy has been widely used in surface coating, adhesives, encapsulants for semiconductor, and insulating materials for electric devices due to their toughness, low shrinkage on cure, outstanding adhesion, and chemical resistance.[5,10–12] Beside, one drawback for epoxy is retardancy properties. Therefore, improvement of thermal properties of epoxy has been widely investigated. POSS can be incorporated into the polymers by covalent bonds and/or physical blending. Although compatibility between POSS and epoxy can be improved by covalent bonds, this results in a homogeneous distribution of inorganic in the organic phase, and therefore, results in good charring properties of the nanocomposite materials.[13] Phase separation of POSS/epoxy nanocomposite occurs when POSS-diamine is added to the epoxy, indicating that even prereaction of a monofunctional POSS exhibited influence on morphology of nanocomposite. In addition, the effect of the type and reactivity of functional groups in the POSS affected the phase and thermomechanical properties in the cured epoxy hybrid. Similarly, Laine and coworkers pointed out that the small changes in nanoscale architecture of epoxy nanocomposite can significantly affect the macroscale properties.[14–16]

The sulfone epoxy (SEP) monomer compound was prepared according to previous literature.[17] In this work, various weight ratios of isocyanate-type POSS (isocyanatopropyldimethylsilyl-isobutyl-POSS, IPI-POSS) were incorporated into the SEP monomer to prepare side chain-type SEP/POSS nanocomposites.

Additionally, the dispersed morphology of the inorganic POSS moieties was investigated via scanning electron microscopy (SEM) and transmission electron microscopy. The thermal degradation properties of the various SEP/POSS nanocomposites were investigated via thermogravimetric analysis (TGA) and the different thermal calculation parameters such as the statistic heat-resistant index temperature (T_s), apparent decomposition temperature (T_A), heat-resistant index (T_{zg}), integral procedure decomposition temperature (IPDT), and thermal decomposition activation energy (E_a) were calculated using the Horowitz–Metzger integral method.

EXPERIMENT

Materials

The 4,4-methylenedianiline supplied by Acros Organic Co., Belgium, was used as the curing agent. The SEP monomer was prepared according to our previous study.[15] Isocyanatopropyldimethylsilyl-isobutyl-POSS (IPI-POSS; chemical formula, $C_{34}H_{75}NO_{14}Si_9$; molar mass, 974.73 g/mol) bearing seven isobutyl groups and one isocyanate group was procured from Hybrid Plastics, Fountain Valley, CA. Tetrahydrofuran (THF) was obtained from Tedia Co., OH.

Instrumental methods

Fourier transform infrared spectra (FT-IR) were measured with a Perkin–Elmer Spectrum FT-IR 2000 (Perkin–Elmer Co., USA). The cured nanocomposites were measured with a Perkin–Elmer Spectrum One FT-IR equipped with an attenuated total reflectance accessory. The morphology of the fracture surface of the composite was examined using a JEOL JSM-5300 scanning electron microscope (SEM). The energy dispersive X-ray (EDX) was used to investigate the distribution of Si atoms in the hybrid creamers. The EDX measurements were conducted with a JEOL JSM-5300 micro analyzer. Differential scanning calorimetry (DSC) thermograms were recorded with a thermal analyzer DSC-Q10 (Waters Co., MA) at optimum heating rates of 10°C/min in open air. The air flow rate was 50 mL/min. TGA was performed using a thermal analyzer TGA-951 (Waters Co.) at a heating rate of 10°C/min in a nitrogen atmosphere.

Preparation of the SEP/POSS nanocomposites

The various SEP/POSS nanocomposites were prepared with different weight ratios of IPI-POSS (0, 1, 3, 5, 7, 9 wt %), keeping a 2 : 1.1M ratio of the SEP to DMA curing agent. The SEP-3IP is the SEP/POSS nanocomposite, which possesses 3 wt % IPI-POSS. Meanwhile, all the reactants were mixed and dis-
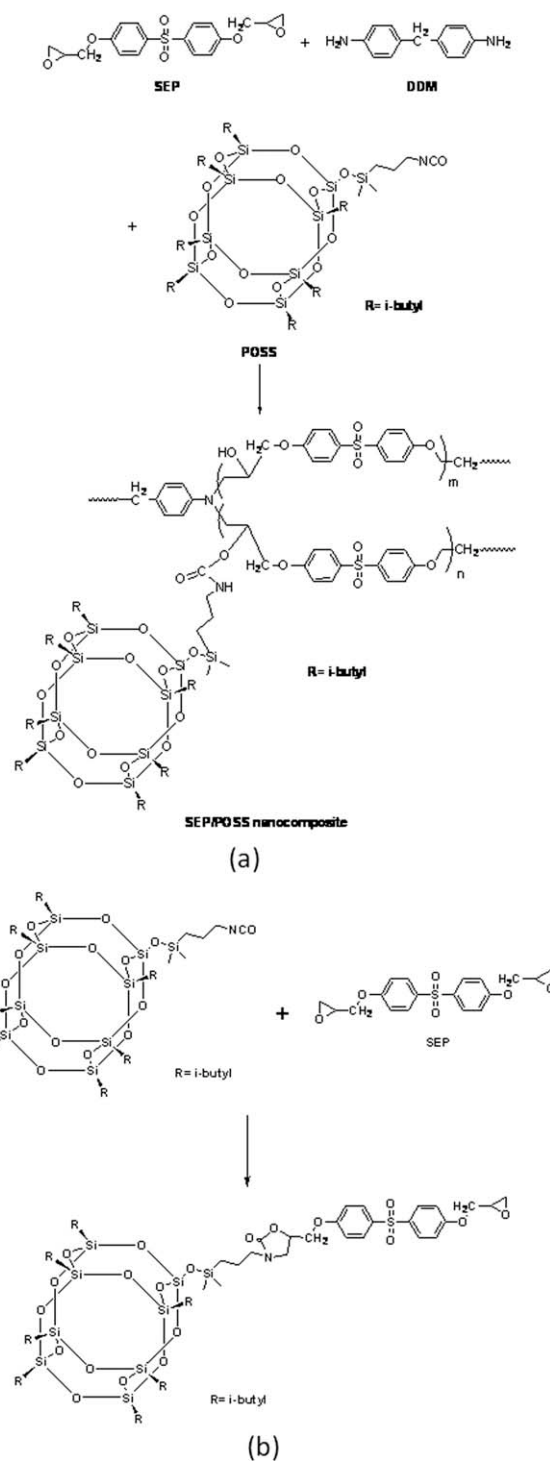
Scheme 1 (a) Isocyanate group of POSS reacted with hydroxyl group in SEP/DMA polymer, (b) isocyanate group of POSS reacted with epoxy group of SEP.

solved homogeneously in the THF at room temperature. The solvent was removed under vacuum at RT (24 h) and the residue was then heated at 80°C (2 h), 120°C (2 h), 160°C (4 h), and 180°C (6 h). The preparation reaction is demonstrated in Scheme 1.
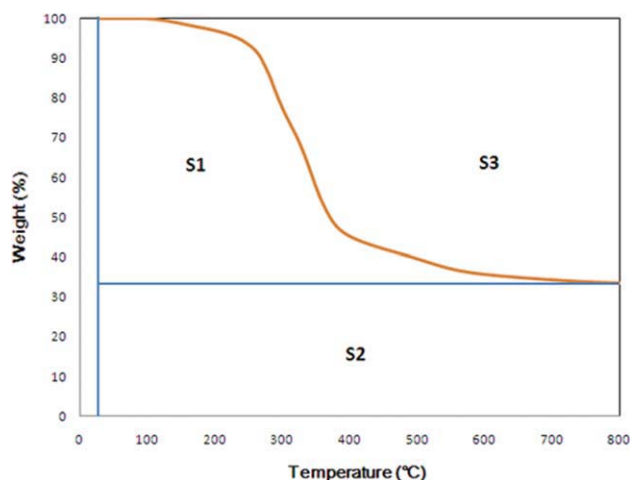
Figure 1 Schematic representation of S_1, S_2, and S_3 for calculating A and K in IPDT. [Color figure can be viewed in the online issue, which is available at wileyonlinelibrary.com.]

The integral procedure decomposition temperature (IPDT)[16–18]

The IPDT was calculated by the method proposed by a previous investigation[18–20] and is shown in eq. (1):

$$IPDT(^{\circ}C) = AK \cdot (T_f - T_i) + T_i \qquad (1)$$

where A is the area ratio of the total experimental curve defined by the total TGA thermogram traces. T_i is the initial experimental temperature, and T_f is the final experimental temperature. In this study, the T_i and T_f were 50 and 800°C, respectively. A and K can be calculated by eqs. (2) and (3). The values of S_1, S_2, and S_3 were determined by previous studies.

$$A = \frac{S_1 + S_2}{S_1 + S_2 + S_3} \qquad (2)$$

$$K = \frac{S_1 + S_2}{S_1} \qquad (3)$$

where A and K are the area ratios of total experimental curve defined in TGA thermogram. Figure 1 shows a representation of S_1, S_2, and S_3.

The activation energies of thermal decomposition (E_a)[17–19]

The activation energies of thermal decomposition were obtained from the TGA decomposed trace and calculated from the Horowitz–Metzger integral method by eq. (4).

$$\ln[\ln(1 - \alpha)^{-1}] = \frac{E_a \times \theta}{R \times T_{max}^2} \qquad (4)$$

In eq. (4), E_a is the activation energy of the thermal decomposition, and α is the thermal decomposition

fraction. T_{max} is defined as the temperature at the maximum rate of weight loss of thermal decomposition. θ and R are the $T - T_{max}$ and gas constant, respectively. Furthermore, E_a was determined from the slope of the straight line corresponding to the plot of $\ln\{\ln(1 - \alpha)^{-1}\}$ versus θ.

The statistic heat-resistant index (T_s)[21–24]

The statistic heat-resistant index temperature (T_s) was determined from the temperature of 5% weight loss (T_{d5}) and of 30% weight loss (T_{d30}) of the sample by TGA. The statistic heat-resistant index temperature (T_s) was calculated by the following eq. (5):

$$T_s = 0.49[Td_5 + 0.6 * (Td_{30} - Td_5)] \qquad (5)$$

The apparent decomposition temperature (T_A) and the heat-resistant index (T_{zg})[25]

The T_A and the heat-resistant index (T_{zg}) were calculated from the eqs. (6) and (7), respectively.

$$T_A = (10C - 3B)/7 \qquad (6)$$

$$T_{zg} = (T_A + B)/2x \qquad (7)$$

In eqs. (6) and (7), the parameters B and C were determined from the TGA trace, which represented the temperature of 50 wt % weight loss (T_{d50}) and the temperature of 15 wt % weight loss (T_{d15}), respectively. Additionally, the parameter x is the functionality index. When the epoxy content was above 50%, the parameter x of the epoxy compound was 2.37. However, when the epoxy content was below 50%, the parameter x of the nonepoxy compound was 2.14. In this work, the parameter x was 2.37, since the epoxy contents were higher than 50%.

RESULTS AND DISCUSSION

Synthesis of the SEP/POSS nanocomposites

Figure 2 presents the FT-IR spectra of the SEP-9IP nanocomposite and IPI-POSS, respectively. The FT-IR data reveal that the IPI-POSS has the NCO characteristic peak at 2268 cm^{-1}. However, this characteristic peak disappeared in the FT-IR spectra of the SEP-9IP nanocomposite, because the NCO group reacted with the hydroxyl group in the oxirane ring opening.[26] Possible reaction mechanism of SEP/POSS is illustrated in Scheme 1. Scheme 1(a) showed that SEP and DMA form the epoxy polymer first, following the isocyanate of POSS reacted with hydroxyl group of SEP in side chain. The characteristic peak at 1739 cm^{-1} can be assigned as carbonyl group vibration in the carbamate structure. Because
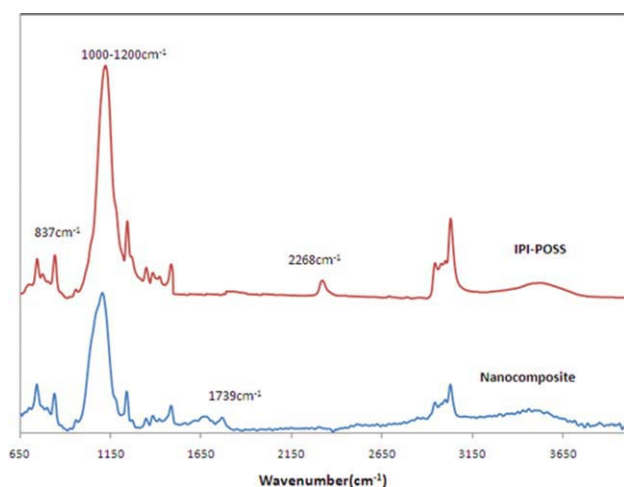
Figure 2 FT-IR spectra of IPI-POSS and SEP-9IP nanocomposite. [Color figure can be viewed in the online issue, which is available at wileyonlinelibrary.com.]

of the low isocyanate concentration in the SEP/POSS nanocomposite (9 wt % of POSS in POSS/SEP), only a weak carbonyl vibration was observed in FT-IR spectrum. According to previous literature,[27] reaction of isocyanate of POSS and epoxy also gives a one-to-one addition compound, and form oxazolidono linkage between the POSS and SEP as shown in Scheme 1(b). The same carbamate structure appears in the oxazolidono ring, making it difficult to identify the main reaction mechanism in POSS/SEP/DMA nanocomposite systems. We can conclude the chemical linkage form within the nanocomposite. Meanwhile, the characteristic peak of siloxane of the POSS (Si—O—Si asymmetric strength) appeared between 1000 and 1200 cm^{-1}, and exhibits a broad characteristic pattern. The characteristic peak was observed at 837 cm^{-1}, which is associated with the Si—CH$_3$ rocking bonding.[28,29]

The morphology of the SEP/POSS nanocomposites

SEM microphotograph indicates that the SEP/POSS nanocomposite dispersed homogeneously and uniformly in the epoxy.[30] Because the POSS functional group possessed good reactivity with the polymer matrix,[31] the silicon elements are distributed evenly and without any aggregation in the SEP/POSS nanocomposite [as shown in Fig. 3(a,b)]. POSS domains were dispersed uniformly in the epoxy matrix.[32,33]

The glass transition temperature (T_g) of the SEP/POSS nanocomposites

Table I indicates that the glass transition temperature (T_g) decreased with the IPI-POSS content. The SEP/POSS nanocomposites possess bulky IPI-POSS segments side chains, which not only improve the polymer chain mobility but also increase the free

volume. The bulky IPI-POSS moieties might disturb the curing reaction and the crosslinking architecture.[34] Consequently, the T_gs of various SEP/POSS nanocomposites were lower than that of the pristine SEP. Kopesky et al. and Iacono et al.[35,36] found that the POSS domains may generate the plasticizing effect, which could decrease the T_g.

The thermal degradation properties of the SEP/POSS nanocomposites

In our previous investigation,[15] the sulfone group of SEP could be degraded at lower temperature to generate the sulfate derivatives char. Moreover, the sulfate derivatives char might improve the thermal stability of polymer matrices.[15,37] Figure 4 and Table I indicate that the T_{d5} values of various SEP/POSS nanocomposites were lower than that of pristine SEP. Since the IPI-POSS side chains contain organic alkyl groups (*i*-butyl groups) and the thermally unstable urethane-like group, the bulky POSS side chains may disturb the curing reactions and generate

(a)
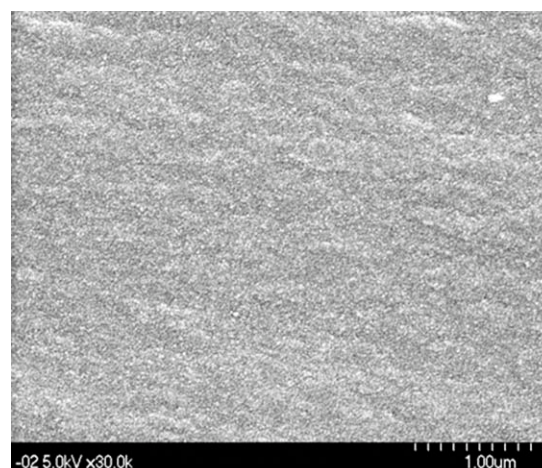
(b)

Figure 3 (a) SEM microphotography, (b) Si-mapping microphotography.

TABLE I
Thermal Degradation Properties of the Various SEP/POSS Nanocomposites

Sample	T_{d5}[a] (°C)	$Char_{800}$[a] (%)	T_{d5}[b] (°C)	$Char_{800}$[b] (%)	T_g (°C)
SEP-0IP	278	39.68	284.63	1.12	164
SEP-1IP	233	31.38	239.16	1.34	126
SEP-3IP	189	30.37	199.39	1.70	111
SEP-5IP	207	33.57	193.71	2.07	108
SEP-7IP	195	30.83	189.26	2.91	106
SEP-9IP	236	30.28	206.44	3.99	105

[a] Under the nitrogen atmosphere.
[b] Under the air atmosphere.

the oligomer in the curing reaction. Tamaki et al.[38] found that the poor polymerization reactivity might decrease the thermal stability.

Fina et al.[39] indicated that the initial thermal decomposition and evaporation of the i-butyl POSS occurred at about 200°C, and the primary carbon atom of the i-butyl POSS possessed higher reactivity toward oxygen. In nitrogen atmosphere, the char yield of various SEP/POSS nanocomposites were lower than that of pristine SEP because of the POSS fragments sublimation and evaporation when they were heated above the POSS melting temperature.[39] In open air, although, low solid residue in all SEP/POSS can be ascribed the intermediate product of SEP/POSS still decomposed at high temperature. The char yields of SEP/POSS nanocomposites increased with the IPI-POSS content and were higher than that of pristine SEP. Song et al.[40] indicated that the polysiloxanes were oxidized and decomposed at high temperature to form the silicon dioxide and a few free carbons products. Liu and Lee[41] found that the POSS could generate thermally stable SiO_x compounds and improve the char yield of nanocomposites. Therefore, the char yield of SEP was lower than other SEP/POSS nanocomposites in open air. The increased char yield could reduce the amounts of combustible gases evolved during the thermal degradation and improve the flame retardancy.[42]

Tables II and III present the five parameters of thermal degradation properties, such as the statistic heat-resistant index temperature (T_s), the T_A, the heat-resistant index (T_{zg}), the IPDT, and the thermal decomposition activation energies (E_a), respectively. T_s, T_A, and T_{zg} of the SEP/POSS nanocomposites were lower than those of the pristine SEP. Fu et al.[25] indicated that the poor crosslinking architectures could decrease the T_A, T_{zg}, and the initial degradation temperature (T_{IDT}) values. The bulky POSS side chain may disturb the SEP curing reaction and generate the oligomer compounds, leading to the destruction of the crosslinking architectures of the nanocomposites. The T_s values were determined from the T_{d5} and T_{d30}, which are temperature pa-

rameters correlated with the T_{IDT} and crosslinking architectures.

The SEP/POSS nanocomposites contain oligomer, which could destroy the crosslinking architectures of curing reaction. The phenomenon could cause degradation at low temperature and reduce the IPDT slightly. However, the IPDT values increased with
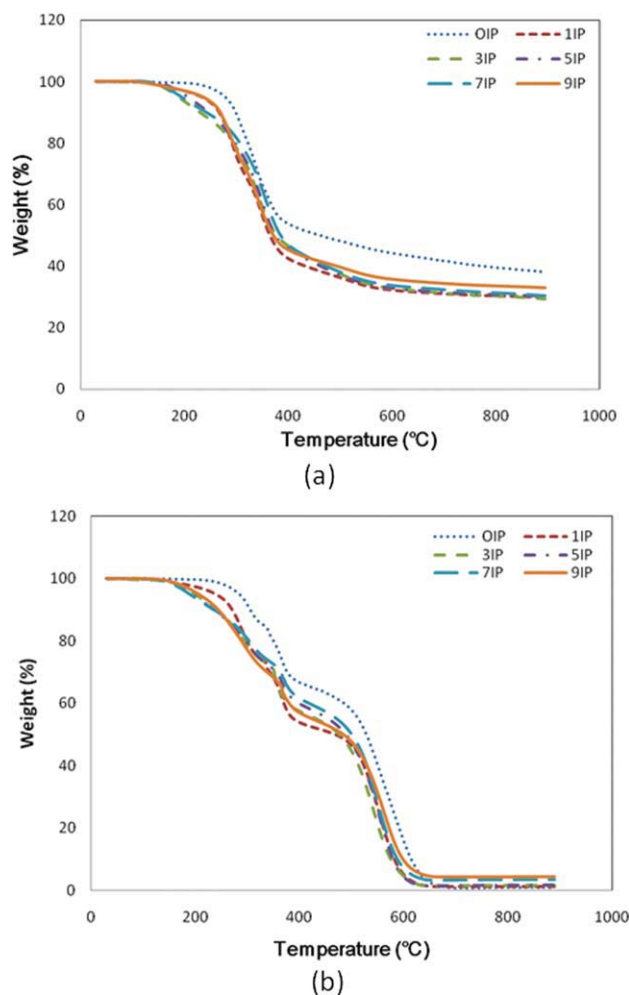

Figure 4 TGA thermal analysis of various SEP/POSS nanocomposites (a) under nitrogen atmosphere, (b) under air atmosphere. [Color figure can be viewed in the online issue, which is available at wileyonlinelibrary.com.]

TABLE II
Thermal Degradation Parameters of the Various SEP/POSS Nanocomposites Under the Nitrogen Atmosphere

Sample	T_S (°C)	T_A (°C)	T_{zg} (°C)	E_a (kJ/mol)	IPDT
SEP-0IP	155.18	245.85	149.36	75.17	1455.75
SEP-1IP	138.72	247.00	129.20	43.87	1010.04
SEP-3IP	133.46	222.84	126.90	48.45	1053.28
SEP-5IP	137.97	235.93	129.15	50.20	1028.75
SEP-7IP	137.98	240.52	132.23	51.66	1052.91
SEP-9IP	141.32	246.30	130.47	47.02	1113.49

TABLE III
Thermal Degradation Parameters of Various SEP/POSS Nanocomposites Under the Air Atmosphere

Sample	T_S (°C)	T_A (°C)	T_{zg} (°C)	E_{a1} (kJ/mol)	E_{a2} (kJ/mol)	IPDT
SEP-0IP	166.56	247.77	163.89	57.80	81.20	495.30
SEP-1IP	147.83	207.74	142.69	46.34	90.66	414.08
SEP-3IP	142.54	183.84	139.30	46.14	89.31	425.85
SEP-5IP	142.55	176.65	140.61	33.15	93.84	416.61
SEP-7IP	144.30	181.25	143.88	33.39	88.02	444.23
SEP-9IP	139.86	175.07	139.21	34.41	77.49	453.68

IPI-POSS content, which is associated with the generation of the silicon dioxide char yield.

In a nitrogen atmosphere, the E_a of various SEP/POSS nanocomposites were similar to the other parameters of thermal degradation properties, because the alkyl groups of the POSSs and oligomers easily decomposed at lower temperatures. However, for SEP-1IP–SEP-9IP, the E_a increased with the POSS content, which is associated with the nanoreinforcement effect of the POSS.[43]

Figure 4(b) presents two thermal degradation stages in open air. The activation energies of thermal degradation of the first thermal degradation stage (E_{a1}) and the second thermal degradation stage (E_{a2}) are summarized in Table III. The oxygen of the air could act as reaction partner with the alkyl group's decomposition of the POSS and the thermal degradation of the oligomers at low temperature, which in turn decreased the E_{a1}. However, the E_{a2}s of various SEP/POSS nanocomposites were higher than that of the pristine SEP. The second thermal degradation stage consists of the volatilization, decomposition, condensation, and oxidation reactions.[40] Therefore, the E_{a2} values showed no tendency from SEP-1IP to SEP-9IP. The apparent rise of E_{a2} from SEP-0IP to SEP-7IP can be ascribed to the decomposition of intermediates formed from the degradation of SEP/POSS during the first stage.

CONCLUSION

The SEP/POSS nanocomposites were prepared using isocyanatopropyl-dimethylsilyl-isobutyl-POSS (IPI-POSS) and the SEP, which possessed the bulky

POSS side chains. There was no large aggregation observed and the POSS domains were dispersed uniformly in the epoxy matrix. The glass transition temperature (T_g) decreased with the IPI-POSS content, because the bulky POSS side chains could not only generate the oligomers but also interrupt the network architectures in the curing reaction. This phenomenon also resulted in decreasing of the initial thermal degradation temperature. In the beginning of thermal degradation of epoxy matrix in air, POSS reacts with alkyl and aromatic structure from SEP and form the intermediate product of POSS/SEP. Therefore, the activation energies of second thermal degradation stage increased from 81.2 to 93.84 kJ/mol in open air (SEP-0IP–SEP-7IP). Eventually, the intermediate product of POSS/SEP decomposed with increase in the temperature. The increased char yield from SEP-0IP~ SEP-9IP revealed that POSS/epoxy nanocomposite materials exhibited higher flame retardancy properties than sole epoxy.

References

1. Li, G. Z.; Wang, L.; Toghiani, H.; Daulton, T. L.; Koyama, K.; Pittman, C. U., Jr. Macromolecules 2001, 34, 8686.
2. Xu, H.; Kuo, S. W.; Lee, J. S.; Chang, F. C. Polymer 2002, 43, 5117.
3. Brus, J.; Urbanová, M.; Strachota, A. Macromolecules 2008, 41, 372.
4. Lee, A.; Lichtenhan, J. D. Macromolecules 1998, 31, 4970.
5. Choi, J.; Kim, S. G.; Laine, R. M. Macromolecules 2004, 37, 99.
6. Liu, Y. L.; Liu, C. S.; Cho, C. I.; Hwu, M. J. Nanotechnology 2007, 18, 1.
7. Xu, H.; Yang, B.; Wang, J.; Guang, S.; Li, C. J Polym Sci Part A: Polym Chem 2007, 45, 5308.
8. Liu, H.; Zheng, S. Macromol Rapid Commun 2005, 26, 196.

 9. Song, X. Y.; Geng, H. P.; Li, Q. F. Polymer 2006, 47, 3049.
10. Wang, C. S.; Lin, C. H. J Appl Polym Sci 2000, 75, 429.
11. Wei, Q.; Lazzeri, A.; Cuia, F. D.; Scalari, M.; Galoppini, E. Macromol Chem Phys 2004, 205, 2089.
12. Chen, G. H.; Yang, B.; Wang, Y. Z. J Appl Polym Sci 2006, 102, 4978.
13. Su, C. H.; Chiu, Y. P.; Teng, C. C.; Chiang, C. L. J Polym Res 2010, 17, 673.
14. Choi, J.; Harcup, J.; Yee, A. F.; Zhu, Q.; Laine, R. M. J Am Chem Soc 2001, 123, 11420.
15. Choi, J.; Yee, A. F.; Laine, R. M. Macromolecules 2003, 36, 5666.
16. Sellinger, A.; Laine, R. M. Chem Mater 1996, 8, 1592.
17. Chiu, Y. C.; Chou, I. C.; Tseng, W. C.; Ma, C. C. M. Polym Degrad Stab 2008, 93, 668.
18. Doyle, C. D. Anal Chem 1961, 3, 77.
19. Park, S. J.; Cho, M. S. J Mater Sci 2000, 35, 3525.
20. Wu, C. S.; Liu, Y. L.; Chiu, Y. C.; Chiu, Y. S. Polym Degrad Stab 2002, 78, 41.
21. Horowitz, H. H.; Metzger, G. Anal Chem 1963, 35, 1464.
22. Lehrle, R. S.; Williams, R. J. Macromolecules 1994, 27, 3782.
23. Grimbley, M. R.; Lehrle, R. S. Polym Degrad Stab 1995, 19, 223.
24. Jiang, B.; Hao, J.; Wang, W.; Jiang, L.; Cai, X. Eur Polym Mater 2001, 37, 463.
25. Fu, J.; Shi, L.; Chen, Y.; Yuan, S.; Wu, J.; Lian, X.; Zhong, Q. J Appl Polym Sci 2008, 109, 340.
26. Solomons, T. W. G. Fundamental of Organic Chemistry, 5th ed.; Wiley: New York, 1997, p 788.
27. Smith, D. A. Nature 1963, 197, 285.
28. Markovic, E.; Clarke, S.; Matisons, J.; Simon, G. P. Macromolecules 2008, 41, 1685.
29. Hagiwara, Y.; Shimojima, A.; Kuroda, K. Chem Mater 2008, 20, 1147.
30. Kim, K. M.; Adachi, K.; Chujo, Y. Polymer 2002, 43, 1171.
31. Li, W.; Liu, F.; Wei, L.; Zhao, T. J Appl Polym Sci 2007, 104, 3903.
32. Chou, C. H.; Hsu, S. L.; Yeh, S. W.; Wang, H. S.; Wei, K. H. Macromolecules 2005, 38, 9117.
33. Chou, C. H.; Hsu, S. L.; Dinakaran, K.; Chiu, M. Y.; Wei, K. H. Macromolecules 2005, 38, 745.
34. Chiu, Y. C.; Ma, C. C. M.; Liu, F. Y.; Chiang, C. L.; Riang, L.; Yang, J. C. Eur Polym Mater 2008, 44, 1003.
35. Kopesky, E. T.; Haddad, T. S.; McKinley, G. H.; Cohen, R. E. Polymer 2005, 46, 4743.
36. Iacono, S. T.; Budy, S. M.; Mabry, J. M.; Smith, D. W., Jr. Macromolecules 2007, 40, 9517.
37. Lin, J. F.; Ho, C. F.; Huang, S. K. Polym Degrad Stab 2000, 67, 137.
38. Tamaki, R.; Choi, J.; Laine, R. M. Chem Mater 2003, 15, 793.
39. Fina, A.; Tabuani, D.; Carniato, F.; Frache, A.; Boccaleri, E.; Camino, G. Thermochim Acta 2006, 440, 36.
40. Song, L.; He, Q.; Hu, Y.; Chen, H.; Liu, L. Polym Degrad Stab 2008, 93, 627.
41. Liu, Y. L.; Lee, H. C. J Polym Sci Part A: Polym Chem 2006, 44, 4632.
42. Liu, Y. L.; Chou, C. I. Polym Degrad Stab 2005, 90, 515.
43. Liu, Y. R.; Huang, Y. D.; Liu, L. Compos Sci Technol 2007, 67, 2864.